Safety and preliminary efficacy of pembrolizumab following trans-arterial chemoembolization for hepatocellular carcinoma: the PETAL phase Ib study.

David J. Pinato[1,2*], Antonio D'Alessio[1,2*], Claudia Angela Maria Fulgenzi[1*], Alexandra Emilia Schlaak[3*], Ciro Celsa[1,4], Saskia Killmer[3], Jesus Miguens Blanco[5], Caroline Ward[1], Charalampos-Vlasios Stikas[1], Mark R. Openshaw[6], Nicole Acuti[1], Georgios Nteliopoulos[1], Cristina Balcells[1], Hector C. Keun[1], Robert D. Goldin[7], Paul J. Ross[8,9], Alessio Cortellini[1,10], Robert Thomas[11], Anna-Mary Young[12], Nathan Danckert[5], Paul Tait[11], Julian R. Marchesi[5], Bertram Bengsch[3,13,14†], Rohini Sharma[1†]

1. Department of Surgery & Cancer, Faculty of Medicine, Imperial College London, Hammersmith Hospital, Du Cane Road, W120HS London, UK.
2. Division of Oncology, Department of Translational Medicine, University of Piemonte Orientale, Novara, Italy.
3. Department of Internal Medicine, University Hospital Freiburg, 79106 Freiburg, Germany.
4. Section of Gastroenterology & Hepatology, Department of Health Promotion, Mother and Child Care, Internal Medicine and Medical Specialties, PROMISE, University of Palermo, Palermo, Italy.
5. Department of Metabolism, Digestion and Reproduction, Faculty of Medicine, Imperial College London, St Mary's Hospital Campus, London, UK
6. Institute of Cancer and Genomics Sciences, University of Birmingham, Birmingham, UK.
7. Centre for Pathology, Imperial College London, Charing Cross Hospital, Fulham Palace Road, London, UK.
8. Department of Medical Oncology, Guy's & St Thomas' NHS Foundation Trust, London, SE19RT, UK.
9. King's College Hospital NHS Foundation Trust, London, SE5 9RS, UK.
10. Division of Medical Oncology, Policlinico Universitario Campus Bio-Medico, Rome, Italy
11. Interventional Radiology, Imperial College NHS Trust, Hammersmith Hospital, Du Cane Road, W120NN, London, UK.
12. Department of Medical Oncology, St Georges University Hospitals, NHS Foundation Trust, St George's University Hospitals NHS Foundation Trust, Blackshaw Road, SW17 0QT London, UK.
13. Signalling Research Centres BIOSS and CIBSS, University of Freiburg, Freiburg, Germany.
14. German Cancer Consortium (DKTK), Heidelberg, Germany, partner site Freiburg.

Word Count: 4993 **Tables:** 2 **Figures:** 4

Running Title: TACE and Pembrolizumab in HCC.

Keywords: HCC, TACE, immunotherapy, PD-1.

* Denotes equal contribution as joint first authorship.
† Denotes joint senior authorship.

To whom correspondence should be addressed:

Dr David J. Pinato, MD MRes MRCP PhD
Clinical Reader and Consultant in Medical Oncology
Imperial College London Hammersmith Campus,
Du Cane Road, W12 0HS, London (UK)
Tel: +44 020 83833720 E-mail: david.pinato@imperial.ac.uk

Statement of translational relevance

PETAL is the first early-phase clinical trial testing the hypothesis of synergy between transarterial chemoembolization (TACE) and sequential PD-1 targeted immunotherapy for liver-confined hepatocellular carcinoma (HCC). With the growing interest in the use of immune checkpoint inhibitors in the early stages for HCC, PETAL confirms the feasibility of the combined approach between ICI and locoregional treatments, supporting their ongoing investigation in larger, randomised phase III trials.

Abstract.

Background. TACE may prime adaptive immunity and enhance immunotherapy efficacy. PETAL evaluated safety, preliminary activity of TACE plus pembrolizumab and explored mechanisms of efficacy.

Methods. Patients with liver-confined HCC were planned to receive up to 2 rounds of TACE followed by pembrolizumab 200 mg every 21 days commencing 30-days post-TACE until disease progression or unacceptable toxicity for up to 1 year. Primary endpoint was safety, 21-days dose-limiting toxicities (DLT) from pembrolizumab initiation. Secondary endpoints included progression-free survival (PFS) and evaluation of tumour and host determinants of response.

Results. Fifteen patients were included in the safety and efficacy population: 73% had non-viral cirrhosis, median age was 72 years. Child-Pugh (CP) class was A in 14 patients. Median tumour size was 4 cm. Ten patients (67%) received pembrolizumab after 1 TACE, 5 patients after 2 (33%). Pembrolizumab yielded no synergistic toxicity nor DLTs post-TACE. Treatment-related adverse events occurred in 93% of patients most commonly skin rash (40%), fatigue and diarrhoea (27%). After a median follow-up of 38.5 months, objective response rate (ORR) 12 weeks post-TACE was 53%. PFS rate at 12 weeks was 93% and median PFS was 8.95 months (95%CI 7.30-NA). Median duration of response was 7.3 months (95%CI: 6.3-8.3). Median OS

was 33.5 months (95%CI: 11.6-NA). Dynamic changes in peripheral T-cell subsets, circulating tumour DNA, serum metabolites and in stool bacterial profiles highlight potential mechanisms of action of multi-modal therapy.

Conclusions. TACE plus pembrolizumab was tolerable with no evidence of synergistic toxicity, encouraging further clinical development of immunotherapy alongside TACE.

Introduction.

Patients presenting with liver-confined HCC, preserved liver function and good performance status cluster into “intermediate stage” or Barcelona Clinic Liver Cancer (BCLC) B stage(1). In this patient subgroup, where overall survival (OS) often extends beyond 2 years, guidelines recommend trans-arterial chemoembolization (TACE) with the intent of prolonging OS by achieving local tumour control and prevent systemic spread of the disease(2).

The efficacy of TACE relies on the dual ischemic and cytotoxic effect stemming from the sequential intra-arterial delivery of cytotoxic chemotherapy followed by direct occlusion of the arterial neo-vascular supply to the tumour. Clinically, this translates into radiologically measured responses in 35% of patients, which associates with a 14% improvement of patients’ survival at 2-years(3). Whilst the therapeutic landscape of advanced HCC has recognized a number of advancements, management of BCLC B HCC has marginally shifted since demonstration of benefit of TACE over placebo in the early 2000s(4). Whilst combination of TACE with sorafenib might counteract tumour progression in selected patients(5), the lack of a convincing OS benefit(6, 7) in association with synergistic toxicity seen from combination of certain anti-angiogenics with TACE(8) calls for the development novel therapeutic combinations to improve patient outcomes in this highly heterogeneous stage of HCC. Immune checkpoint inhibitors (ICI) targeting the programmed-cell death 1 (PD-1) pathway are effective in a proportion of patients with HCC and now constitute a global standard of care for the treatment of unresectable/advanced HCC, having been demonstrated non inferior to sorafenib as monotherapy in certain trials or superior when administered in association with Vascular Endothelial Growth Factor (VEGF) targeting antibodies or with Cytotoxic T-Lymphocyte Antigen-4 (CTLA-4)(9).

The demonstrated efficacy of ICI in advanced HCC has placed increasing emphasis on the

immune-modulatory role of loco-regional therapies for HCC(10) (11, 12) (13). Innate and adaptive immune activation are key prognostic determinants in patients undergoing loco-regional therapies including TACE, with chronic modulation of the T-helper-2 lymphocyte response(10, 14-16) and regulatory T-cells(17) being associated with clinical outcome after successful local treatment.

The clinical hypothesis underlying this early-phase clinical study is that TACE may act as a loco-regional inducer of immunogenic cell death, enabling sequential treatment with the anti-PD-1 antibody pembrolizumab to promote effective immune reconstitution and improve anti-tumour control. This study aims to characterize safety, preliminary efficacy of TACE plus pembrolizumab and to explore mechanisms of efficacy using multiple validated readouts of host immunity.

Methods.

Study design and participants.

PETAL is a prospective, open-label, single arm phase Ib trial of pembrolizumab in combination with TACE in patients with liver-confined HCC. The study protocol has been previously published(18). This trial was conducted at tertiary referral centres for the care of HCC (Imperial College, King's College and St. George's Hospital) in London, United Kingdom. Eligible patients were aged $\geq$18 years, had confirmed radiologic diagnosis of HCC based on the American Association for the Study of Liver Diseases (AASLD) criteria(19), were ineligible to liver resection, transplantation and naïve to systemic therapy. At screening, patients were required to have at least one previously untreated lesion (i.e., the TACE-amenable lesion) measurable disease by Response Evaluation Criteria in Solid Tumours (RECIST) v1.1, an Eastern Cooperative Oncology Group (ECOG) performance status of 0-1; adequate organ function (haematology, coagulation, blood chemistry and hepato-renal function) and a Child Pugh (CP)

Class score ≤7. Patients with extrahepatic metastases, hepatic encephalopathy, diuretic-refractory ascites or history of bleedingwere excluded. Full inclusion/exclusion criteria and representativeness of study population are listed in **Supplementary Table S1-2**.

The study was conducted in accordance with Good Clinical Practice and the Declarations of Helsinki and Istanbul. Study protocol and subsequent amendments were approved by the London Westminster Research Ethics Committee (Reference 17/LO/1180, EudraCT 2017-000471-85, NCT03397654) and the UK Health Research Authority. All patients provided written informed consent prior to participation.

Study Procedures.

PETAL was conducted in 2 parts. Study part 1 consisted of a safety run-in of up to 6 participants treated with pembrolizumab administered intravenously over 30 minutes at the dose of 200 mg every 3 weeks (Q3W) at the pre-defined interval of 30 days (+3 days) post-TACE. Subjects in part 1 were observed for determination of dose-limiting toxicities (DLT), with a particular focus on the emergence of any liver-related AEs defined as per system-organ class (SOC) designation occurring over a 21-days' time window from Cycle 1 of pembrolizumab, with weekly laboratory assessments in Cycle 1 only. All patients in study part 1 received conventional super-selective TACE, consisting in intra-arterial injection of lipiodol plus doxorubicin (60 mg fixed dose) followed by injection of an embolic agent (gelfoam) to arrest blood flow to the tumour. Following completion of Part 1 and upon confirmation of safety of the conventional (c)TACE/pembrolizumab combination, patients in Part 2 were allowed to have either cTACE or drug eluting beads (DEB) TACE with up to 300-500μ LC Beads™ mixed with 150 mg of doxorubicin. Patients achieving incomplete de-vascularisation 4 weeks after initial TACE were considered for a second procedure by treating investigators. Patients requiring >1 TACE were mandated to receive the same type of procedure (either cTACE or cTACE / DEB-TACE if in Part

2) and be reassessed for response beginning 4 weeks after second TACE and commence pembrolizumab thereafter. However, after completion of 2 TACE procedures all patients who remained eligible by clinical and laboratory features were dosed with pembrolizumab not earlier than 30 (+3) from the second procedure irrespective of radiologic response to TACE. Tumour reassessments were planned with dynamic CT or MRI 4 weeks after each TACE procedure and subsequently after 4 cycles of pembrolizumab and continuing every 12 weeks thereafter until end of study. Pembrolizumab was continued until oncological disease progression, unacceptable toxicity or completion of 1 year of treatment. **Fig.1A** highlights the study flow chart.

Outcomes.

The primary study endpoint was to assess safety and tolerability of pembrolizumab following TACE and to determine whether pembrolizumab following TACE could lead to DLT events. Safety assessments included physical and laboratory findings and adverse events (AEs) were defined according to the National Cancer Institute (NCI) Common Toxicity Criteria for Adverse Events (CTCAE) version 4.0. Patients were assessed for the emergence of AEs before starting immunotherapy (within 30 days post TACE for the first part and within 45 days post TACE in part 2) and then every week for the first 21 days and every 3 weeks thereafter for part 1; every 3 weeks from cycle 1 for part 2. The causality between AEs and treatment was assigned by the investigators. Patients were assessed for the emergence of AEs up to 30 days after end of treatment. A DLT was defined as a treatment-related $\geq$grade 3 AE occurring during the assessment window of 21 days from the first administration of pembrolizumab. With safety being primary study endpoint, no power calculation for hypothesis testing was required to formally power the study and the upper 95% confidence interval for toxicity events was used to inform decision to proceed to a subsequent efficacy study. Alongside primary safety analyses, an exploratory analysis was performed to obtain preliminary data on the efficacy of the TACE

plus pembrolizumab combination. Tumour response was assessed using RECIST v1.1 criteria at screening, 4 weeks after each TACE procedure and 12-weekly during pembrolizumab treatment. To capture the combined efficacy ot TACE plus pembrolizumab we elected as primary efficacy outcomes the evaluating radiological overall response rates (ORR) at 12 weeks after last TACE, alongside progression-free survival (PFS) and overall survival (OS).

ORR was defined as the percentage of patients reporting either partial response (PR) or complete response (CR) at the first scan at 12 weeks after the last TACE. Median duration of response was defined as the time from first complete response (CR) or pathological response (PR) to death or progression in those achieving an objective response.

PFS was defined by the time from last TACE to the first occurrence of documented disease progression based on RECIST v1.1 criteria or death from any cause, whichever occurred first, and it was calculated using Kaplan-Meier. A PFS rate at 12 weeks was calculated as the percentage of patients free from death or progression at 12 weeks from last TACE using the Kaplan-Meier method. OS was defined from the time of last TACE until death from any cause. PFS was censored at the time of last tumour assessment in those patients who had not progressed by the time of database lock, whereas OS was censored at the time of last patient contact. Survival follow-up was carried out every 8 weeks after end of treatment. Median follow-up was calculated using reverse Kaplan-Meier method from screening to last follow-up. All patients who received at least one dose of pembrolizumab were included in the safety and efficacy analyses.

Quality of Life (QoL) Measures.

Health-related quality of life (HRQoL) was evaluated using the European Organisation for Research and Treatment of Cancer (EORTC) Quality-of-life Questionnaire Core 30 (QLQ-C30) and the EORTC Quality-of-life Questionnaire-Hepatocellular Carcinoma 18 (QLQ-HCC18)(20).

Further details are reported in **Supplementary Method S1.**

Biomarker Assessments.

The comprehensive translational program included analyses on circulating tumour DNA (ctDNA) (**Supplementary Figures S1-2**), peripheral T-cell repertoire, peripheral immune population phenotyping with mass cytometry (**Supplementary Figure S3 and Tables S3-4**), targeted transcriptomics on bulk RNA extracted from screening biopsies, stool metataxonomics and serum metabolomic profiling (**Supplementary Table S5**). The detailed methods can be found in **Supplementary Methods S2-9.**

Data Availability Statement.

The data generated in this study are available upon request from the corresponding author. The sequencing data are not publicly available due to patient privacy requirements but are available upon reasonable request from the corresponding author.

Statistical Analyses.

Statistical analyses were performed using SPSS version 25.0 (IBM Inc., Chicago, IL, USA) and GraphPad PRISM (GraphPad software inc., La Jolla, CA, USA) unless stated otherwise, with all estimates being reported with corresponding 95% confidence intervals and a two-tailed level of significance of $p<0.05$.

Results.

Patient Characteristics.

Patient allocation is highlighted in **Fig.1A**. From February 2018 to September 2022, 26 patients provided consent and were screened for the study. At the time of database lock (28th February 2023), 15 patients had received at least one dose of pembrolizumab and completed the DLT period. Patient features at screening are presented in **Table 1**. Median age of the safety-evaluable population was 72 years (IQR: 63.5-75.5), most of the patients were male (73.3%), had liver cirrhosis (73.3%) of non-viral origin (73.4%) and an ECOG performance status of 0 (60.0%). One patient with CP B liver class was enrolled in the safety run-in-phase, and the remaining scored A (66.6% CP 5 and 26.6% CP 6). All patients had liver-confined HCC: the majority had 1 single neoplastic nodule (53.3%), with a median maximum tumour diameter of 4 cm (IQR: 3.4-4.5). Most patients were treatment-naïve for HCC, with only 1 patient (9%) having received prior radiofrequency ablation to an unrelated lesion.

Safety and Quality of Life.

In the 6 patients enrolled in study part 1, no DLTs were observed from the combination of TACE with pembrolizumab in the 21-days following first pembrolizumab administration. One patient who commenced treatment with CP B7 functional class discontinued treatment after completion of DLT window due to treatment-unrelated worsening of liver functional reserve (grade 1 bilirubin increase from baseline and grade 2 ascites). Following the independent data safety monitoring committee review, the protocol was amended to continue recruitment to CP A disease patients only.

Throughout the observation period, 14 patients (93.3%) developed at least 1 adverse event (AE) of any grade, and 7 (46.7%) grade 3 or higher. No grade 4 or 5 AEs were reported. As described in **Table 2**, fatigue and anorexia were the most reported AEs, occurring in 10

participants (66.7%), followed by skin rash (60.0%) and diarrhoea (53.3%). Fourteen patients (93.3%) experienced at least one treatment-related toxicity (TRAE) of any grade. Skin rash was the most common TRAE (40.0%), followed by diarrhoea, pruritus, and fatigue occurring in 4 participants each (26.7%, **Supplementary Table S6)**. The only grade 3 TRAE reported, skin rash (6.7%) required oral corticosteroid treatment and subsequently resolved allowing treatment resumption. Sequential administration of pembrolizumab after TACE did not result in unexpected hepatic toxicity as supported by longitudinal liver function tests (**Supplementary Figure S4**).

Mean scores for global health status (GHS)/Quality of Life (QOL) and functioning domains on EORTC QLQ-C30 questionnaire and for symptom scales on EORTC QLQ-C30 and QLQ-HCC18 questionnaires at baseline and at the end of treatment are reported in **Supplementary Table S7** and **Supplementary Figures S5 and S6**, showing a favourable trend in most domains. Mean changes from baseline in GHS/QoL and functioning domains are showed in **Supplementary Figure S7**.

Efficacy.

At data cut-off, 15 patients were evaluable for efficacy: 10 (66.7%) had received one round of TACE, whereas and 5 (33.3%) had required 2 procedures prior to starting immunotherapy. Tumour assessment performed 4 weeks after TACE and before pembrolizumab initiation demonstrated that 6 patients achieved complete response to TACE (40%), 2 had a partial response (13.3%) and 7 patients (46.7%) achieved radiological stable disease as best response to TACE.

Pembrolizumab was commenced in all patients at least 30 (+3) days after TACE (median 1.05 months, IQR 1.00-1.35). Median duration of pembrolizumab treatment was 3.1 months (IQR 1.5-5.1) and median number of administered cycles was 5 (IQR 3.0-7.5).

After a median follow up of 38.5 months (95%CI, 24.7-52.5), all 15 patients had stopped immunotherapy. Radiologically proven disease progression was the most common cause of pembrolizumab cessation occurring in 7 (46.7%) subjects, after a median of 5 cycles (IQR 3.0-6.8). Other causes for premature pembrolizumab discontinuation included treatment-unrelated progression of liver dysfunction (n=2), grade 3 diarrhoea secondary to *Clostridium difficile* infection (n=1), treatment-related persisting grade 2 peripheral neuropathy (n=1), COVID-19 pandemic (n=2) and withdrawal of consent (n=1). A Swimmer's plot summarizing these events and their timing is showed in **Fig.1B**.

At the time of data cut-off, the PFS rate at 12 weeks from the last TACE was 93.3% (95%CI: 0.82-1.00), and median PFS from last TACE was 8.95 months (95%CI: 7.30-NA, **Fig.1C**). ORR at 12 weeks from last TACE was 53.3% and included 2 PR and 6 CR. Median duration of response was 7.3 months (95%CI: 6.3-8.3). By the time of data cut-off, 10 patients had died, with a median OS of 33.5 months (95%CI: 11.5-NA) from enrollment. The 6-months and 1 year OS rates were 93.3% (95%CI: 0.82-1.00) and 70% (0.49-0.99), respectively **(Fig.1D).**

Circulating Tumour DNA and T-cell receptor repertoire.

We performed a tumour-informed ctDNA analysis using a bespoke panel validated by our group (21) in all patients with quantifiable cell-free (cfDNA) in peripheral plasma in at least one timepoint. We sequenced the cfDNA extracted from a total of 28 timepoints, and 10 patients were considered eligible, of whom four achieved a radiological response at 12 weeks (40%).
Baseline characteristics are summarised in **Supplementary Table S8**. At screening, cfDNA was detectable at the median concentration of 0.57 ng/μL (IQR, 0.46-0.72), of which ctDNA accounted for a median of 8.5% (IQR 4.2-17.6). While cfDNA at screening did not differ across responders and non-responders (median 0.73 vs 0.57 ng/ μL, p=0.25), baseline ctDNA was significantly higher in responders (median 0.15 vs 0.06 ng/ μL, p=0.01; **Fig.2A**).

When longitudinally analysing ctDNA across timepoints, we observed that the radiological response was recapitulated by the evolution of ctDNA concentration. In fact, ctDNA concentration significantly decreased during ICI treatment in responders (median 0.15 vs 0.07 ng/ µL at screening and on treatment respectively, p=0.0048), while a significant increase was observed in non-responders from screening to EOT (median 0.06 vs 0.08 ng/ µL, p=0.003 (**Fig.2A**).

Most frequent mutated gene was ARID1A (41% of samples), followed by PI3KCA (33%) and HNF1A (22%, **Fig.2B-C**). For patients with an available paired assessment, the VAF of ARID1A appeared to dynamically follow the course of the treatment, with a decrease on-treatment and an increase upon treatment failure (**Supplementary Figure S8A**). Both in samples of responders and non-responders, the VAF of specific variants mirrored the evolution of the treatment, with a clearance after TACE and an increase at treatment failure (**Supplementary Figure S8B-C**).

We investigated whether the TCR-b repertoire underwent any modifications across the different timepoints, and whether it was associated with the achievement of radiological response at 12 weeks. We found that TACE did not significantly impact on clonality, even after subdividing per response (**Supplementary Figure S9 A-C**), and we did not find any significant change in clonality induced by ICI administration (**Supplementary Figure S9 D-F**). However, when looking at the TCR-b repertoire prior to ICI commencement, we observed a significantly higher productive Simpson clonality in responders, as also shown by the frequency of the top 10 rearrangements (**Fig.2 D-E**), with no difference in entropy (**Supplementary Figure S10 A-B**).

Peripheral Immune Phenotyping.

We used highly multiplexed mass cytometry (CyTOF) for immune monitoring and longitudinal phenotyping of peripheral blood mononuclear cells isolated at multiple timepoints: screening

(i.e. pre-TACE), pre-pembrolizumab, at cycle 5 of pembrolizumab and at the EOT. In total, 13 out of 15 patients were evaluable for analysis. Data analysis was performed based on gating of n=30 predefined immune cell populations **(Supplementary Figure S3)** and via an unbiased data-driven clustering pipeline.

We investigated dynamic changes of immune cell subpopulations along the study, and we correlated the findings with the achievement of radiological response after 12 weeks, in keeping with the secondary clinical endpoint. Interestingly, when comparing the immune subpopulations at screening and at treatment discontinuation, we observed a significant enrichment in CD8+ CXCR5-CCR4+CXCR3-CCR6-Tc2 at EOT compared to baseline (**Fig.3 A-B**). Screening for possible predictors of immunotherapy response, we observed that CD8+ CXCR5-CCR4-CXCR3+CCR6- Tc1 cells were significantly more represented in non-responders compared to responders prior to ICI initiation (**Fig.3C**). At the EOT, a significant increase in CD3-CD19+ B cells was observed in non-responders (**Fig.3D**). In sum, while overall the data indicate limited variation in the broad immune profile, individual immune cell subsets were linked to treatment efficacy.

We thus focused our analysis on the heterogeneity of T cell responses using a data-driven high-dimensional clustering approach. CD45+CD3+CD19- T cells were sampled from non-responder and responder patients and the T cell landscape was visualized using tSNE dimension reduction **(Fig.4A)**. As expected, Tc1 and Tc2 cells identified as differentially expressed in our prior predefined analysis also differed in their localization on the T cell map in areas associated with different outcomes (**Fig.4B-C).** Our data-driven clustering approach further revealed 12 distinct subsets of T cells in the patient cohort (**Fig.4D**). Notably, two T cell subsets prior to ICI therapy, cluster c07 and cluster c08, were associated with differential patient outcomes: cluster c08 was enriched in patients who responded to therapy, while cluster c07 was enriched in non-responders **(Fig.4E).** Phenotypic analysis informed c07 as an early differentiated memory CD4+

T cell cluster, whereas c08 represented a Th1-like CD4 T cell cluster with high levels of T-bet, CX3CR1, KLRG1 and CD57 (**Fig.4F**). These data suggest that presence of a Th1-polarised T cell response prior to anti-PD-1 checkpoint therapy is associated with the achievement of response to treatment.

Targeted Transcriptomics of baseline tumour biopsies.

We performed bulk targeted transcriptomic analyses on total RNA purified from 10 pre-treatment biopsies obtained at screening that satisfied quality control criteria. In exploratory analyses, we compared differences in the expression of 770 genes related to adaptive and innate immunity (Nanostring Pancancer Immune panel) in 4 responders and 6 non-responders **(Supplementary Figure S11A)**. Samples from patients achieving a response to TACE plus pembrolizumab were enriched for gene expression signatures reflective of innate immunity including cytokine and chemokine secretion and regulation of macrophage function **(Supplementary Figure S11B)**. Differential gene expression analysis highlighted transcripts involved in the inflammatory process such as FN1, SPP1 and LBP (**Supplementary Figure S12A-B**).

Stool Bacterial Profiles and Metabolic phenotyping.

The microbiota-evaluable population (MEP) consisted of 9 patients, with available paired stool samples. After filtering for the presence of adequate count of sequencing reads, we included 6 patients, whose baseline characteristics can be found in **Supplementary Table S9.** Most prevalent genus at baseline was *Bacteroides* (**Supplementary Figure S13**), with no significant changes in alpha and beta diversity measures across screening and EOT timepoints (**Supplementary Figure S14A-D**). We identified a significant enrichment in the *Clostridium* genus in stool samples at screening, while *Alistipes* was found to be significantly increased at treatment discontinuation (**Supplementary Figure S14E**).

We included in the metabolomics analysis 23 serum samples, collected from 11 patients at three different timepoints: at screening (prior to TACE), prior to pembrolizumab commencement (C1W0), and at the end of treatment (EOT). Baseline characteristics of these patients can be found in **Supplementary Table S10.** When comparing samples collected at screening and at EOT, we found a significant higher abundance of several acyl-carnitines at screening, while the ratio of tyrosine/phenylalanine was significantly increased at the EOT (**Supplementary Figure S15A**).

Data on response to treatment at 12 weeks were available for 8 patients. Sera of responders was found to be significantly enriched in two acyl-carnitines and four phosphatidylcholine lipids (PCaa), while the ratio of methionine-sulfoxide/methionine and the ratio of total acylcarnitine derivatives of dicarboxylic acids (AC-DC)/total acyl-carnitines were significantly increased in non-responders (**Supplementary Figure S15B**).

Discussion.

It has been recognized for a long time that local therapy may evoke significant immunologic consequences in patients with HCC. Local and systemic secretion of pro-inflammatory cytokines and danger-associated molecular patterns (DAMPs) following successful tumour chemoembolization has a priming effect on adaptive immunity(22). Patients who mount a spontaneous CD4 and CD8 response following TACE exhibit improved survival outcomes, underscoring immune modulation as a fundamental mechanism underlying the efficacy of TACE(10, 14-16). Therapeutic combinations between loco-regional and systemic immunotherapies are at the focus of intense research efforts(23).

In this phase Ib study, the combination of TACE plus pembrolizumab was well tolerated and did not lead to synergistic toxicity or unexpected safety concerns. Most TRAEs were grade 1 or 2 and entirely attributable to pembrolizumab exposure with rates and intensity of AEs that are comparable with anti-PD-1/PD-L1 monotherapy use in advanced HCC (14% in KEYNOTE-394 for pembrolizumab, 15% in RATIONALE-208 for tislelizumab, and 6.4% in HIMALAYA for durvalumab)(24-26). Within our study, particular scrutiny was placed on hepatic TRAEs as events of clinical interest in the context of this multi-modal therapeutic approach. Reassuringly, serial evaluation of liver function tests demonstrated no evidence of treatment-related worsening liver dysfunction in the context of the TACE plus pembrolizumab sequential combination.

Establishing a tolerable multimodal therapy is of paramount importance in patients with HCC. Earlier clinical experience in the combination of TACE with the VEGF inhibitor bevacizumab had shown evidence of life threatening adverse events, justifying interruption of clinical development(8). The choice of sequential introduction of pembrolizumab 30 days after TACE, justified by evidence suggesting optimal recovery of liver function tests within 4 weeks from the loco-regional therapy, allowed us to optimally delineate acutely emerging toxicities from the two

therapies and evaluate the relative contribution of each component of multimodal therapy to the overall treatment efficacy. To complement safety data, our analysis of patient reported outcomes portrays substantial stability across multiple validated indices describing of patients' QoL. As demonstrated in advanced HCC, QoL preservation plays an important role in the definition of an appropriate benefit/risk profile from initiation of systemic therapy(27). Our findings, although limited by small sample size, are informative to the onward clinical development of immunotherapy alongside TACE by showing that integration of PD-1 inhibition does not lead to worsening of patients' QoL: a concept that should be further tested in randomized phase III studies.

Anti-tumour activity of pembrolizumab following TACE appeared encouraging in our study, with over 93% of patients remaining progression-free 12-weeks post treatment and for a median duration of 10.3 months. Despite the lack of a control arm, patients achieving a response to the TACE plus pembrolizumab combination achieved durable responses, lasting for a median interval of 7.3 months. By the time of data cut-off, the median OS of our cohort was 33.9 months. Whether sequential exposure to pembrolizumab following TACE may lead to a significant survival advantage in patients with intermediate-stage HCC is a research question beyond the scope of our study. However, the OS estimates reached in our study population are encouraging and compare favourably with recently published case series of patients treated with loco-regional therapy(28), further strengthening the case for future research in this segment of the HCC population. Recently, the EMERALD-1 trial has demonstrated durvalumab plus bevacizumab to improve PFS after 16 weeks of TACE + durvalumab concomitant therapy, with no benefit demonstrated from the addition durvalumab monotherapy over placebo(29). Whilst OS data from EMERALD-1 are eagerly awaited, the PFS and OS figures emerging from our study are provocative in suggesting that a proportion of patients may derive benefit from TACE plus PD-1 monotherapy without suffering excessive adverse events. Whether concomitant

versus sequential immunotherapy is preferred in intermediate-HCC is unknown and reporting of the multiple phase III studies in this field will provide clarity as to the best treatment schedule and choice of agents in this field(30).

Understanding the mechanism of action of PD-1 inhibitors in HCC is an area of high unmet need(31), especially given the lack of predictive value for standard biomarker such as PD-L1 immunostaining(32) or tumour mutational burden in HCC(33).

In this study, phenotypic characterisation of the tumoral immune infiltrate in a subset of patients with pre-treatment tumour biopsies available for analysis shows evidence of an association between gene signatures reflective of tumour cell adhesion, matrix remodelling and immune regulation and response to TACE plus pembrolizumab. Amongst the noted up-regulation of selected acute phase reactants such as LBP, FN1 in responders, we found evidence of SPP1 overexpression, an adverse prognostic marker in HCC also known as osteopontin, which contributes to shape an immune tolerogenic microenvironment in HCC(34) through myeloid cell/macrophage polarisation(35) and adversely influences immunotherapy response(36). The positive association between baseline SPP1 expression and response to TACE plus pembrolizumab is particularly interesting as it resonates with retrospective evidence suggesting improved outcomes from TACE in patients harbouring a pro-inflammatory TME(11). Whether TACE plus pembrolizumab efficiently disrupt the myeloid-enriched “tumour immune barrier” associated with immunotherapy resistance(34) should be the focus of pairwise comparison of pre-TACE biopsy material obtained prospectively in randomised cohorts with or without immunotherapy exposure.

Data-driven high-dimensional analysis further identified a Th1-like CD4 T cell subset that was positively associated with response to treatment, while early differentiated memory CD4+ T cell subset was negatively associated with response. Interestingly, the difference in T-cell subsets

was observed prior to ICI commencement, while no significant change induced by TACE was identified.

Of note, a pre-existing CD8 T-cell response is a considered a central pre-requisite for optimal response to PD-1-based immunotherapy(37, 38). Our detailed phenotypic analysis of peripheral blood immune cells further dissected the different CD8 T cell subsets, and we described an opposite association of Tc1 and Tc2 subsets with therapy outcome. The Tc1 subset frequency prior to ICI therapy was negatively associated with outcome. Phenotypic analysis of the Tc1 subset further revealed expression of many severe exhaustion-associated molecules, such as Tox, Eomes, PD-1, suggesting severe exhaustion of this population. In contrast, the Tc2 subset was identified as a positive correlate of overall treatment success, with a reduced expression of exhaustion markers. Interestingly, the Tc2 subset expressed Tcf-1, and Tcf-1+ CD8+ T cells were found to be associated with response to ICI in other malignancies(39).

Effective anti-tumour rejection relies on the complimentary role of IFN-g secreting Tc1 cells and IL-4 and IL-5 secreting Tc2 cell(39). IL-4 and IL-5 are central to both Th2 and Tc2 cell maturation and Th2/Tc2 polarisation has been observed in tumour infiltrating lymphocytes(37) in a positive correlation that mirrors the one found in responding patients to TACE plus pembrolizumab. Interestingly, previous evidence in lung cancer has shown that local anti-tumour therapy with cyberknife or intensity-modulated radiotherapy enhances Th2 and Tc2 responses, drawing an interesting parallel to the immunogenic effect of the TACE plus pembrolizumab observed in our study(40). Whilst preliminary in nature, evidence of a preferential Tc2 following locoregional therapy emphasise the role of T-cell effector function as a mechanism of action of multi-modal therapy in HCC: an original finding that should constitute the basis of the biomarker development plan in larger studies of this kind.

Further insight into the disease-modulating effect of TACE plus pembrolizumab emerge from the

serial analysis of circulating tumour DNA concentration across timepoints. Using targeted next generation sequencing approach, which recapitulates the most common mutational events in HCC(21), we were able to show that the ctDNA evolution in plasma reproduces the radiological response to treatment, with a significant decrease in ctDNA levels in responders, and a significant rise in patients who did not respond to TACE plus pembrolizumab. Whilst our analysis is limited by the lack of a tumour informed approach, longitudinal changes in the variant allelic frequency of key mutational drivers of HCC highlights the potential of ctDNA as a non-invasive biomarker for the therapeutic monitoring of HCC during multi-modal therapy.

Inspired by the growing interest in the gut microbiome and its perturbation as a mechanism of response to immunotherapy in HCC(41-43), our stool bacterial metagenomics and plasma metabolomics revealed significant changes in the abundance of *Clostridium* and *Alistipes* throughout treatment. *Alistipes* is an increasingly characterised genus of the *Bacteroidetes phylum* that has been associated with positive response to immunotherapy in lung cancer(44). Modification in its abundance throughout multi-modal TACE plus pembrolizumab treatment may highlight a positive bi-directional modulation between the gut microbiome and local plus systemic therapy which would be important to validate as mechanism of therapeutic efficacy in larger studies. Unfortunately, the unfolding of the COVID-19 pandemic(45) prevented a systematic collection of serial stool samples in all patients, limiting our ability to explore whether measures of gut microbial diversity could scale with the extent and duration of response in our patients. However, we were able to investigate the peripheral metabolic state of patients with a comprehensive serial phenotyping. Acyl-carnitines are known to be associated with cirrhosis evolution and HCC development(46) and we observed a significant decrease after TACE, as expected(47). Their increased concentration at baseline in responders could be correlated with a different nutritional status, and their association with tolerance to systemic therapy(48) should be explored further in the context of combined treatment strategies with TACE and

immunotherapy.

There are limitations of this study, including limited sample size, lack of a control arm and the deleterious impact of the COVID-19 pandemic, which made recruitment and retention of participants to this investigator-led clinical trial particularly difficult, leading to a reduction in the number of samples available for translational analyses. Despite these limitations, our study has met its primary objective, having demonstrated that the combination of TACE plus pembrolizumab is tolerable, deliverable and characterized by preliminary but convincing evidence of efficacy in patients with intermediate-stage HCC. Our findings represent an important benchmark for the subsequent development of therapeutic combinations in intermediate-stage HCC.

Declarations:

Acknowledgements. DJP is supported by grant funding from the Wellcome Trust Strategic Fund (PS3416), the Associazione Italiana per la Ricerca sul Cancro (AIRC MFAG 25697), the Roger Williams Foundation for Liver Disease (Small Project Grant) and acknowledges grant support from the Cancer Treatment and Research Trust (CTRT), infrastructural support by the Imperial Experimental Cancer Medicine Centre, Imperial College Healthcare NHS Trust Tissue Bank, and the NIHR Imperial Biomedical Research Centre. The views expressed are those of the authors and not necessarily those of the NIHR or the Department of Health and Social Care. AD and JRM are supported by the National Institute for Health Research (NIHR) Imperial BRC, while AD is further supported by grant funding from the European Association for the Study of the Liver (2021 Andrew Burroughs Fellowship) and from Cancer Research UK (RCCPDB-Nov21/100008). CC is funded by the European Union-FESR or FSE, PON Research and Innovation 2014-2020-DM 1062/2021. BB's research is supported by Deutsche Forschungsgemeinschaft (DFG) research grants # 520992132, # 441891347 (OncoEscape), # 390939984 (CIBSS), # 272983813 (TRR179), # 256073931 (IMPATH), # 518316185 (GMCA) and the German Cancer Consortium (DKTK). The study team would like to acknowledge Dr Alexandros Siskos for their assistance with sample processing for metabolomics analyses, Ms Maria Martinez for their administrative support to the study, Ms Naina Patel, Mrs Nona Rama and Mr Ignazio Puccio for their support in sample preparation for transcriptomics analyses.

Funding. This study was supported by funding from Merck Sharpe and Dohme (MSD) as an investigator-initiated study sponsored by Imperial College London. Infrastructure support was provided by the NIHR Imperial Biomedical Research Centre and the NIHR Imperial Clinical Research Facility. The views expressed are those of the author(s) and not necessarily those of the funder, the NIHR or the Department of Health and Social Care. DJP was supported by personal grant funding from the Wellcome Trust Strategic Fund (PS3416).

Ethics approval and consent to participate: Study protocol and subsequent amendments were approved by the London Westminster Research Ethics Committee (Reference 17/LO/1180, EudraCT 2017-000471-85, NCT03397654) and the UK Health Research Authority. All patients provided written informed consent prior to participation to the study.

Competing Interests: DJP received lecture fees from Bayer Healthcare, EISAI, BMS, Roche, Boston Scientific, travel expenses from BMS and Bayer Healthcare; consulting fees for Mina Therapeutics, DaVolterra, Mursla, IPSEN, Exact Sciences, Avamune, EISAI, Roche, Starpharma, LiFT biosciences and Astra Zeneca; received research funding (to institution) from MSD, GSK and BMS. AD received educational support for congress attendance and consultancy fees from Roche and AstraZeneca. CC received speaker fees and advisory board honoraria from AstraZeneca, Eisai, Merck Sharp & Dohme, Ipsen and travel support from Roche. The other authors declare no conflicts of interest.

Authors Contribution.

Study concept and design: DJP.

Experimentation and acquisition of data: CW, MO, NA, GN, CBN, PJR, AMY, JM, SK, AES, RS.

Analysis and interpretation of data: DJP, BB, CAMF, AD, AC, CC, ES, SK, JMB, CW, MO, NA, GN, HK, CB, ND, RDG, PJR, AMY, RT, AC, PT, JM, BB.

Drafting of the manuscript: DJP.

Critical revision of the manuscript for important intellectual content: All the authors.

Statistical analysis: CAMF, AC, AD, DJP.

Obtained funding: DJP.

Administrative, technical, or material support: DJP, BB, RS.

Study supervision: DJP, RS.

Figure Legends.

Figure 1. A. Study flow chart. **B.** Swimmer's plot of study participants receiving TACE plus pembrolizumab. Each bar represents one subject in the study. Depth, duration of response, dates of radiologic response or progressive disease, and presence of ongoing response are indicated accordingly. **C.** Kaplan-Meier curve illustrating the progression-free survival of the study population. **D.** Kaplan-Meier curve illustrating the overall survival of the study population.

Figure 2. A. Dynamic changes of circulating tumour DNA (ctDNA) concentration at various study timepoints and relationship with response to treatment. **B.** Distribution of individual mutations across pre-treatment samples (n=28). **C.** Oncoplot illustrating the distribution and type of mutations identified in pre-treatment plasma samples of patients recruited to the study. Each column represents a sample and each row a different gene. The left barplot illustrates the variant allelic frequency pertaining to each sample, while the right barplot has the frequency of mutations in each gene. The top bar plot estimates the tumour mutational burden (TMB) calculated based on number of mutations per Megabase of sequenced genome. Samples ordered by the most mutated genes. **D**. Distribution of the top 10 T-cell receptor rearrangements as measured by productive frequency prior to pembrolizumab start in responders (n=6) and non responders (n=7) (n=2 not available). **E**. Productive Simpson clonality was significantly higher in responders before commencement of systemic therapy. Abbreviations: ctDNA, circulating-tumour DNA; C1, cycle 1; EOT, end of treatment; VAF, variant allele frequency; ICI, immune checkpoint inhibitors. An asterisk (*) marks a statistically significant difference at $p<0.05$ threshold, two asterisks (**) correspond to $p>0.01$.

Figure 3. A. Heatmap illustrating relative representation of individual cell types as assayed using CyToF across the various study timepoints (Screening, Cycle 1 Week 0 i.e. post-TACE, and end of treatment) stratified on the basis of the achievement of response 12 weeks following TACE plus pembrolizumab combination. Hierarchically clustered heatmap displays mean

frequencies of lymphocyte subsets per timepoint and response to therapy, visualized by z-score based colouring after column normalization. **B**. Tc2 cell frequency differed between screening and EOT (n=8, paired samples) **C.** Tc1 cell frequency before ICI therapy was different between responders (n=6) and non-responders (n=7). **D.** B-cell frequency differed at end of therapy between responders (n=6) and non-responders (n=7). An asterisk (*) marks a statistically significant difference at $p<0.05$ threshold.

Figure 4. A. tSNE visualization of CD45+CD3+CD19- T lymphocytes pooled (top), divided by response to therapy (middle) and in addition by timepoint (bottom). Each dot corresponds to a single cell. Representative data of 4 patients, subsampled up to 15.000 per sample, analysis of 157.543 cells in total. **B.** Overlay plot indicating the localization of Tc1 and Tc2 cells on the tSNE map. **C.** T cell marker expression is visualized on the tSNE map by colour heatmap. **D.** T cells were clustered based on their high-dimensional expression profile using FlowSOM. Clusters are visualized by the indicated colours on the tSNE map**. E.** Cluster abundance of c07 and c08 in responder and non-responder patients. Data are represented as mean with SD and analysed by paired t-test. **F.** Hierarchically clustered heatmap indicating mean marker expression of T cell differentiation, activation and exhaustion markers by each cluster and including manually gated Tc1 and Tc2 subsets as in Figure 3. Expression is visualized by z-score as indicated, data was scaled per column. *$p < 0.05$. **$p < 0.01$.

References.

1. Elshaarawy O, Gomaa A, Omar H, Rewisha E, Waked I. Intermediate stage hepatocellular carcinoma: a summary review. J Hepatocell Carcinoma 2019;6:105-117.

2. Raoul JL, Forner A, Bolondi L, Cheung TT, Kloeckner R, de Baere T. Updated use of TACE for hepatocellular carcinoma treatment: How and when to use it based on clinical evidence. Cancer Treat Rev 2019;72:28-36.

3. Llovet JM, Bruix J. Systematic review of randomized trials for unresectable hepatocellular carcinoma: Chemoembolization improves survival. Hepatology 2003;37:429-442.

4. Llovet JM, Real MI, Montana X, Planas R, Coll S, Aponte J, Ayuso C, et al. Arterial embolisation or chemoembolisation versus symptomatic treatment in patients with unresectable hepatocellular carcinoma: a randomised controlled trial. Lancet 2002;359:1734-1739.

5. Kudo M, Ueshima K, Ikeda M, Torimura T, Tanabe N, Aikata H, Izumi N, et al. Randomised, multicentre prospective trial of transarterial chemoembolisation (TACE) plus sorafenib as compared with TACE alone in patients with hepatocellular carcinoma: TACTICS trial. Gut 2020;69:1492-1501.

6. Lencioni R, Llovet JM, Han G, Tak WY, Yang J, Guglielmi A, Paik SW, et al. Sorafenib or placebo plus TACE with doxorubicin-eluting beads for intermediate stage HCC: The SPACE trial. J Hepatol 2016;64:1090-1098.

7. Meyer T, Fox R, Ma YT, Ross PJ, James MW, Sturgess R, Stubbs C, et al. Sorafenib in combination with transarterial chemoembolisation in patients with unresectable hepatocellular carcinoma (TACE 2): a randomised placebo-controlled,

double-blind, phase 3 trial. Lancet Gastroenterol Hepatol 2017;2:565-575.

8. Pinter M, Ulbrich G, Sieghart W, Kolblinger C, Reiberger T, Li S, Ferlitsch A, et al. Hepatocellular Carcinoma: A Phase II Randomized Controlled Double-Blind Trial of Transarterial Chemoembolization in Combination with Biweekly Intravenous Administration of Bevacizumab or a Placebo. Radiology 2015;277:903-912.

9. Fulgenzi CAM, Scheiner B, Korolewicz J, Stikas CV, Gennari A, Vincenzi B, Openshaw MR, et al. Efficacy and safety of frontline systemic therapy for advanced HCC: A network meta-analysis of landmark phase III trials. JHEP Rep 2023;5:100702.

10. Zerbini A, Pilli M, Penna A, Pelosi G, Schianchi C, Molinari A, Schivazappa S, et al. Radiofrequency thermal ablation of hepatocellular carcinoma liver nodules can activate and enhance tumor-specific T-cell responses. Cancer Res 2006;66:1139-1146.

11. Pinato DJ, Murray SM, Forner A, Kaneko T, Fessas P, Toniutto P, Minguez B, et al. Trans-arterial chemoembolization as a loco-regional inducer of immunogenic cell death in hepatocellular carcinoma: implications for immunotherapy. J Immunother Cancer 2021;9.

12. Flecken T, Schmidt N, Hild S, Gostick E, Drognitz O, Zeiser R, Schemmer P, et al. Immunodominance and functional alterations of tumor-associated antigen-specific CD8+ T-cell responses in hepatocellular carcinoma. Hepatology 2014;59:1415-1426.

13. Rivoltini L, Bhoori S, Camisaschi C, Bergamaschi L, Lalli L, Frati P, Citterio D, et al. Y(90)-radioembolisation in hepatocellular carcinoma induces immune responses calling for early treatment with multiple checkpoint blockers. Gut 2023;72:406-407.

14. Liao Y, Wang B, Huang ZL, Shi M, Yu XJ, Zheng L, Li S, et al. Increased circulating Th17 cells after transarterial chemoembolization correlate with improved

survival in stage III hepatocellular carcinoma: a prospective study. PLoS One 2013;8:e60444.

15. Hiroishi K, Eguchi J, Baba T, Shimazaki T, Ishii S, Hiraide A, Sakaki M, et al. Strong CD8(+) T-cell responses against tumor-associated antigens prolong the recurrence-free interval after tumor treatment in patients with hepatocellular carcinoma. J Gastroenterol 2010;45:451-458.

16. Pinato DJ, Karamanakos G, Arizumi T, Adjogatse D, Kim YW, Stebbing J, Kudo M, et al. Dynamic changes of the inflammation-based index predict mortality following chemoembolisation for hepatocellular carcinoma: a prospective study. Aliment Pharmacol Ther 2014;40:1270-1281.

17. Fu J, Xu D, Liu Z, Shi M, Zhao P, Fu B, Zhang Z, et al. Increased regulatory T cells correlate with CD8 T-cell impairment and poor survival in hepatocellular carcinoma patients. Gastroenterology 2007;132:2328-2339.

18. Fessas P, Scheiner B, D'Alessio A, CA MF, Korolewicz J, Ward C, Tait P, et al. PETAL protocol: a phase Ib study of pembrolizumab after transarterial chemoembolization in hepatocellular carcinoma. Future Oncol 2023;19:499-507.

19. Heimbach JK, Kulik LM, Finn RS, Sirlin CB, Abecassis MM, Roberts LR, Zhu AX, et al. AASLD guidelines for the treatment of hepatocellular carcinoma. Hepatology 2018;67:358-380.

20. Blazeby JM, Currie E, Zee BC, Chie WC, Poon RT, Garden OJ. Development of a questionnaire module to supplement the EORTC QLQ-C30 to assess quality of life in patients with hepatocellular carcinoma, the EORTC QLQ-HCC18. Eur J Cancer 2004;40:2439-2444.

21. Howell J, Atkinson SR, Pinato DJ, Knapp S, Ward C, Minisini R, Burlone ME, et al. Identification of mutations in circulating cell-free tumour DNA as a biomarker in hepatocellular carcinoma. Eur J Cancer 2019;116:56-66.

22. Pol J, Vacchelli E, Aranda F, Castoldi F, Eggermont A, Cremer I, Sautes-Fridman C, et al. Trial Watch: Immunogenic cell death inducers for anticancer chemotherapy. Oncoimmunology 2015;4:e1008866.

23. Foerster F, Galle PR. The Current Landscape of Clinical Trials for Systemic Treatment of HCC. Cancers (Basel) 2021;13.

24. Ren Z, Ducreux M, Abou-Alfa GK, Merle P, Fang W, Edeline J, Li Z, et al. Tislelizumab in Patients with Previously Treated Advanced Hepatocellular Carcinoma (RATIONALE-208): A Multicenter, Non-Randomized, Open-Label, Phase 2 Trial. Liver Cancer 2023;12:72-84.

25. Qin S, Chen Z, Fang W, Ren Z, Xu R, Ryoo BY, Meng Z, et al. Pembrolizumab Versus Placebo as Second-Line Therapy in Patients From Asia With Advanced Hepatocellular Carcinoma: A Randomized, Double-Blind, Phase III Trial. J Clin Oncol 2023;41:1434-1443.

26. Abou-Alfa GK, Lau G, Kudo M, Chan SL, Kelley RK, Furuse J, Sukeepaisarnjaroen W, et al. Tremelimumab plus Durvalumab in Unresectable Hepatocellular Carcinoma. NEJM Evid 2022;1.

27. Galle PR, Finn RS, Qin S, Ikeda M, Zhu AX, Kim TY, Kudo M, et al. Patient-reported outcomes with atezolizumab plus bevacizumab versus sorafenib in patients with unresectable hepatocellular carcinoma (IMbrave150): an open-label, randomised, phase 3 trial. Lancet Oncol 2021;22:991-1001.

28. Han G, Berhane S, Toyoda H, Bettinger D, Elshaarawy O, Chan AWH, Kirstein M, et al. Prediction of Survival Among Patients Receiving Transarterial Chemoembolization for Hepatocellular Carcinoma: A Response-Based Approach. Hepatology 2020;72:198-212.

29. Lencioni R, Kudo M, Erinjeri J, Qin S, Ren Z, Chan S, Arai S, et al. EMERALD-1: A phase 3, randomized, placebo-controlled study of transarterial chemoembolization combined with durvalumab with or without bevacizumab in participants with unresectable hepatocellular carcinoma eligible for embolization. J Clin Oncol 2024;42.

30. Fulgenzi CAM, D'Alessio A, Ogunbiyi O, Demirtas CO, Gennari A, Cortellini A, Sharma R, et al. Novel immunotherapy combinations in clinical trials for hepatocellular carcinoma: will they shape the future treatment landscape? Expert Opin Investig Drugs 2022;31:681-691.

31. Muhammed A, D'Alessio A, Enica A, Talbot T, Fulgenzi CAM, Nteliopoulos G, Goldin RD, et al. Predictive biomarkers of response to immune checkpoint inhibitors in hepatocellular carcinoma. Expert Rev Mol Diagn 2022;22:253-264.

32. Pinato DJ, Mauri FA, Spina P, Cain O, Siddique A, Goldin R, Victor S, et al. Clinical implications of heterogeneity in PD-L1 immunohistochemical detection in hepatocellular carcinoma: the Blueprint-HCC study. Br J Cancer 2019;120:1033-1036.

33. Wong CN, Fessas P, Dominy K, Mauri FA, Kaneko T, Parcq PD, Khorashad J, et al. Qualification of tumour mutational burden by targeted next-generation sequencing as a biomarker in hepatocellular carcinoma. Liver Int 2021;41:192-203.

34. Liu Y, Xun Z, Ma K, Liang S, Li X, Zhou S, Sun L, et al. Identification of a tumour immune barrier in the HCC microenvironment that determines the efficacy of

immunotherapy. J Hepatol 2023;78:770-782.

35. Liu L, Zhang R, Deng J, Dai X, Zhu X, Fu Q, Zhang H, et al. Construction of TME and Identification of crosstalk between malignant cells and macrophages by SPP1 in hepatocellular carcinoma. Cancer Immunol Immunother 2022;71:121-136.

36. Yamauchi R, Ito T, Yoshio S, Yamamoto T, Mizuno K, Ishigami M, Kawashima H, et al. Serum osteopontin predicts the response to atezolizumab plus bevacizumab in patients with hepatocellular carcinoma. J Gastroenterol 2023;58:565-574.

37. Hegde PS, Karanikas V, Evers S. The Where, the When, and the How of Immune Monitoring for Cancer Immunotherapies in the Era of Checkpoint Inhibition. Clin Cancer Res 2016;22:1865-1874.

38. Huang AC, Postow MA, Orlowski RJ, Mick R, Bengsch B, Manne S, Xu W, et al. T-cell invigoration to tumour burden ratio associated with anti-PD-1 response. Nature 2017;545:60-65.

39. Miller BC, Sen DR, Al Abosy R, Bi K, Virkud YV, LaFleur MW, Yates KB, et al. Subsets of exhausted CD8(+) T cells differentially mediate tumor control and respond to checkpoint blockade. Nat Immunol 2019;20:326-336.

40. Huang AC, Postow MA, Orlowski RJ, Mick R, Bengsch B, Manne S, Xu W, et al. T-cell invigoration to tumour burden ratio associated with anti-PD-1 response. Nature 2017;545:60-65.

41. Myojin Y, Greten TF. The Microbiome and Liver Cancer. Cancer J 2023;29:57-60.

42. Pinato DJ, Li X, Mishra-Kalyani P, D'Alessio A, Fulgenzi CAM, Scheiner B, Pinter M, et al. Association between antibiotics and adverse oncological outcomes in patients receiving targeted or immune-based therapy for hepatocellular carcinoma. JHEP Rep

2023;5:100747.

43. Fessas P, Naeem M, Pinter M, Marron TU, Szafron D, Balcar L, Saeed A, et al. Early Antibiotic Exposure Is Not Detrimental to Therapeutic Effect from Immunotherapy in Hepatocellular Carcinoma. Liver Cancer 2021;10:583-592.

44. Jin Y, Dong H, Xia L, Yang Y, Zhu Y, Shen Y, Zheng H, et al. The Diversity of Gut Microbiome is Associated With Favorable Responses to Anti-Programmed Death 1 Immunotherapy in Chinese Patients With NSCLC. J Thorac Oncol 2019;14:1378-1389.

45. Pinato DJ, Zambelli A, Aguilar-Company J, Bower M, Sng C, Salazar R, Bertuzzi A, et al. Clinical portrait of the SARS-CoV-2 epidemic in European cancer patients. Cancer Discov 2020;10:1465-1474.

46. Li S, Gao D, Jiang Y. Function, Detection and Alteration of Acylcarnitine Metabolism in Hepatocellular Carcinoma. Metabolites 2019;9.

47. Iwasa M, Sugimoto R, Ishihara T, Sekoguchi-Fujikawa N, Yoshikawa K, Mifuji-Moroka R, Tanaka H, et al. Usefulness of Levocarnitine and/or Branched-Chain Amino Acids during Invasive Treatment for Hepatocellular Carcinoma. J Nutr Sci Vitaminol (Tokyo) 2015;61:433-440.

48. Okubo H, Ando H, Ishizuka K, Kitagawa R, Okubo S, Saito H, Kokubu S, et al. Carnitine insufficiency is associated with fatigue during lenvatinib treatment in patients with hepatocellular carcinoma. PLoS One 2020;15:e0229772.

Figure 1.

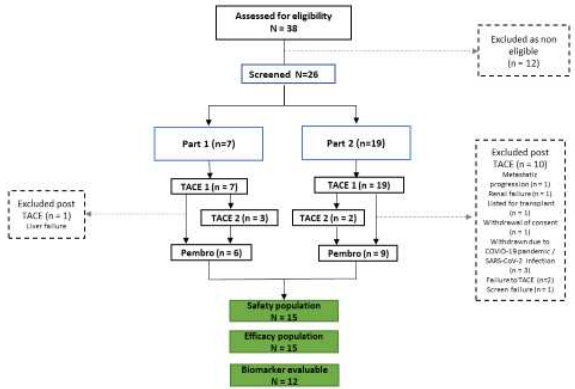

A

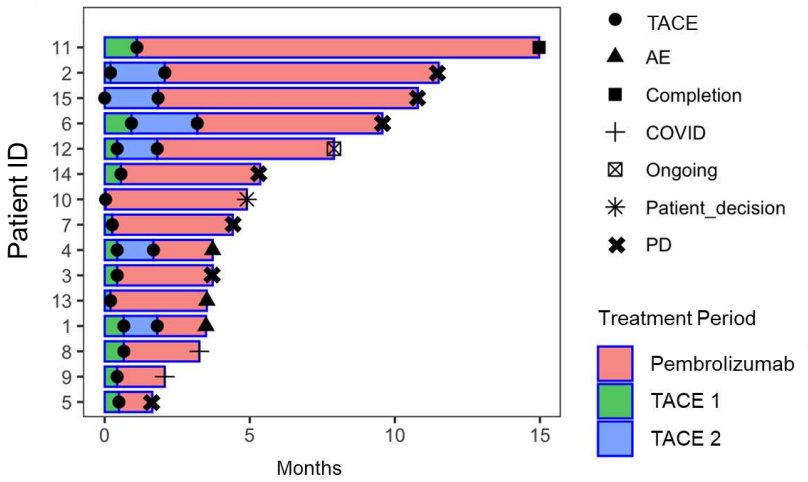

B

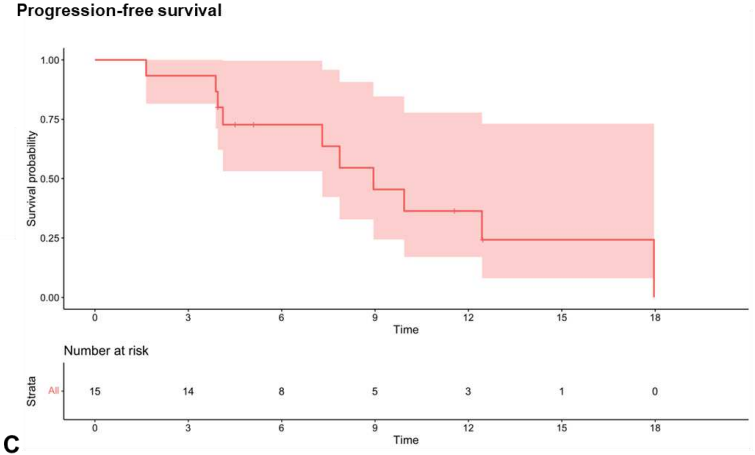

C

PFS rate at 3 months: 93.3% (95%CI: 0.82-1.00)
Median PFS 8.95 months (95%CI: 7.30-NA)

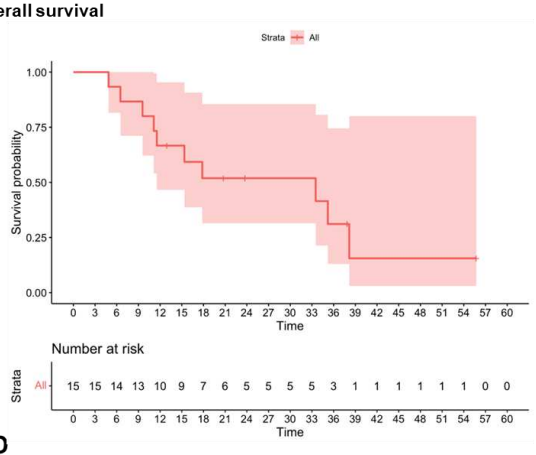

D

Median OS: 33.52 months (95%CI: 11.55-NA)

Figure 2.

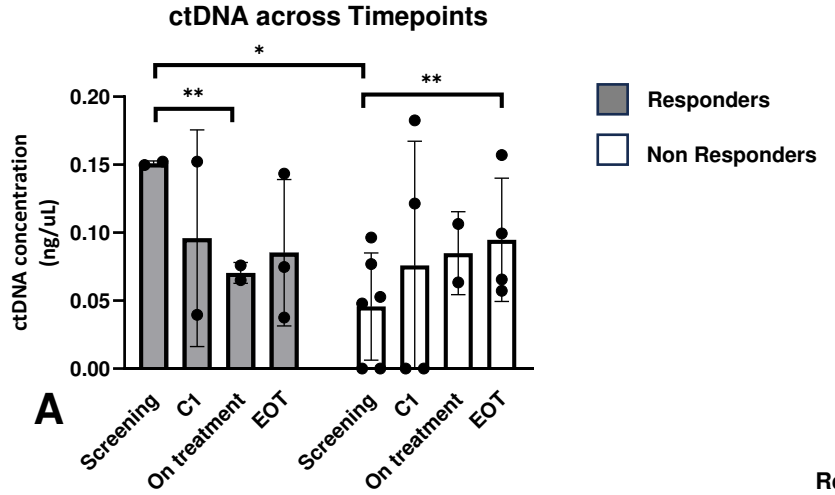

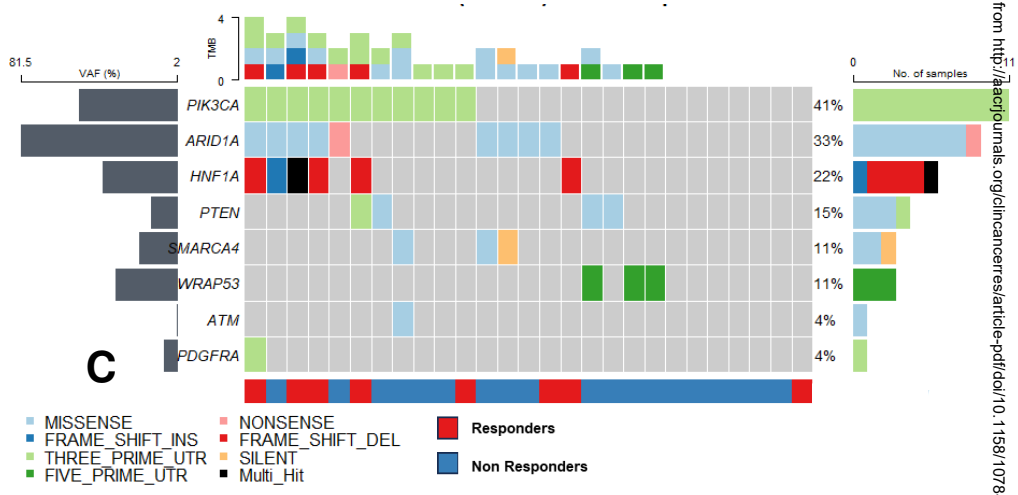

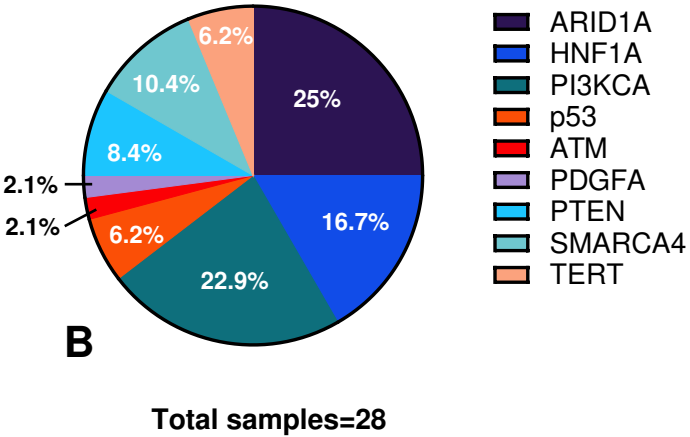

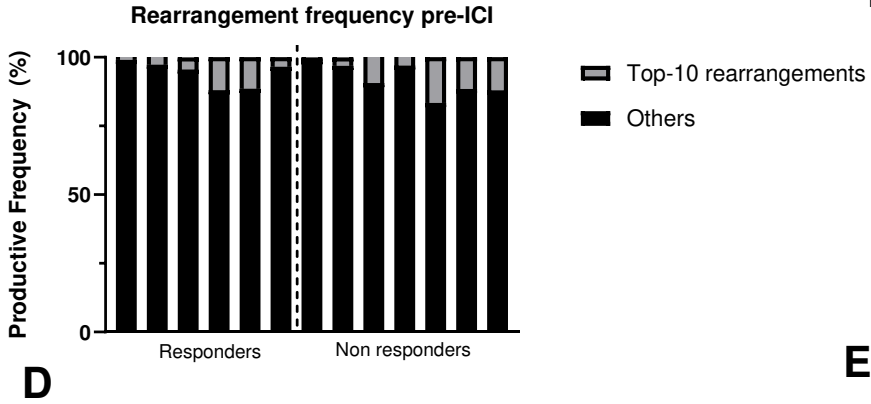

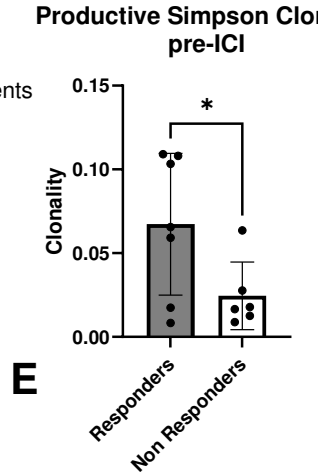

Figure 3.

Figure 4.

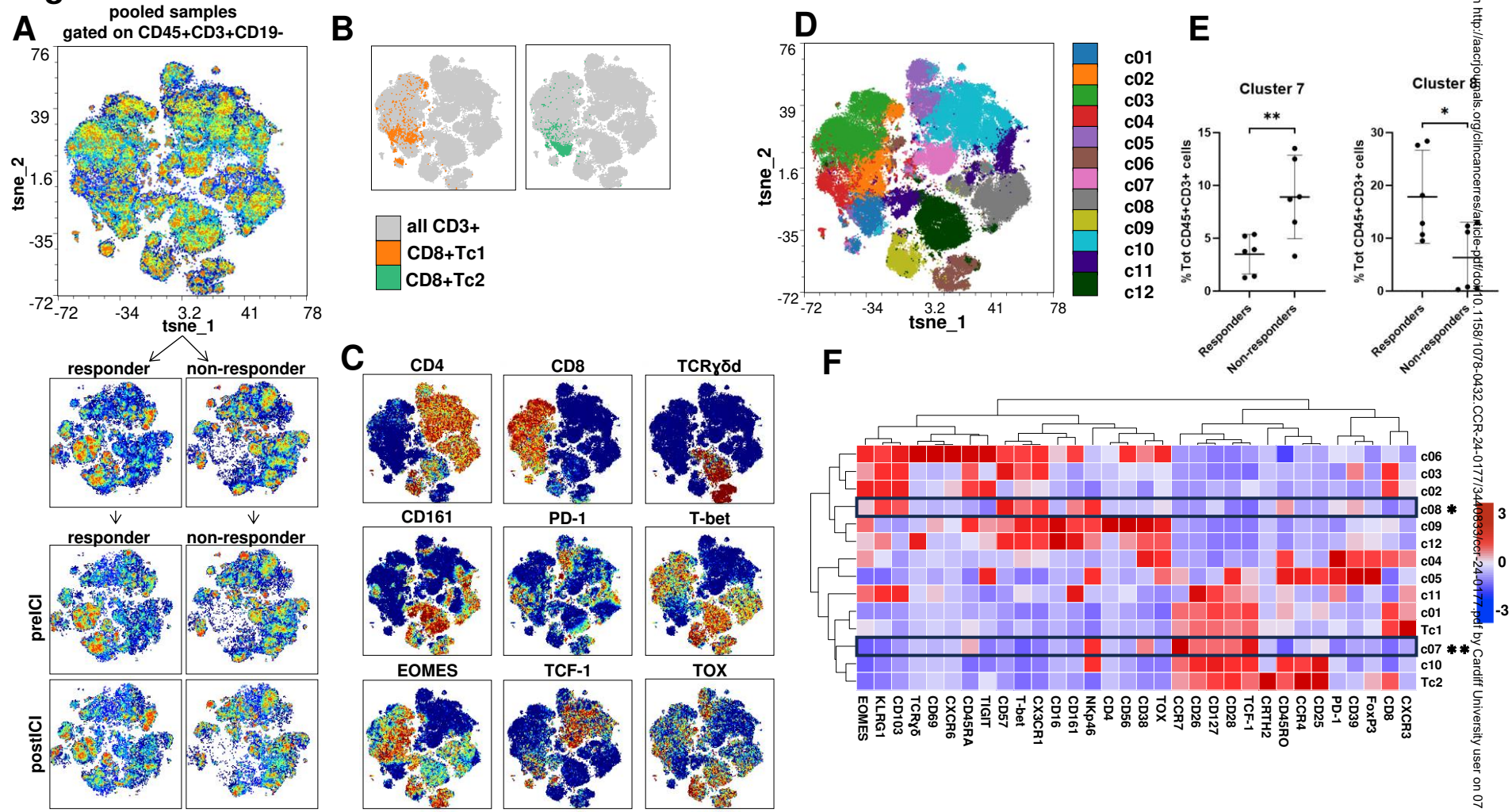

Table 1. Baseline characteristic of the safety-evaluable population.

Age	**Median (IQR)** 72 (63.5-75.5)
Gender Male Female	**N (%)** 11 (73.3%) 4 (26.7%)
Ethnicity White Asian Other (Not stated)	**N (%)** 8 (53.3%) 2 (13.3%) 5 (33.4%)
ECOG PS 0 1	**N (%)** 9 (60.0%) 6 (40.0%)
AFP (ng/ml)	**Median (IQR)** 16 (6.5-37.5)
Child Pugh 5 6 7	**N (%)** 10 (66.6%) 4 (26.6%) 1 (6.8%)
ALBI 1 2	**N (%)** 6 (40.0%) 9 (60.0%)
Cirrhosis Present Absent	**N (%)** 11 (73.3%) 4 (26.7%)
Etiology Viral Non-viral HBV HCV	**N (%)** 4 (26.6%) 11 (73.4%) 2 (13.3%) 2 (13.3%)
BCLC A B	**N (%)** 7 (46.6%) 8 (53.4%)
Number of nodules 1 2 3	**N (%)** 8 (53.3%) 3 (20%) 4 (26.7%)
Maximum diameter (cm)	**Median (IQR)** 4 (3.4-4.5)
Previous surgery Yes No	**N (%)** 0 0
Previous RFA Yes No	**N (%)** 2 (13.3%) 13 (86.7%)
Previous TACE Yes No	**N (%)** 1 (6.6%) 14 (93.4%)

Table 2. All cause Adverse Events occurring in ≥15% of the safety evaluable population.

Adverse Event	Any grade N (%)	Grade ≥3 N (%)
All	14 (93.3%)	7 (46.7%)
Fatigue	10 (66.7%)	1 (6.7%)
Anorexia	10 (66.7%)	1 (6.7%)
Skin-rash	9 (60.0%)	1 (6.7%)
Diarrhoea	8 (53.3%)	1 (6.7%)
Dyspnoea	6 (40.0%)	None
Back pain	6 (40.0%)	None
Pruritus	5 (33.3%)	None
Lethargy	5 (33.3%)	None
Abdominal distension	5 (33.3%)	None
Dry mouth	5 (33.3%)	None
Peripheral oedema	5 (33.3%)	None
Peripheral neuropathy	5 (33.3%)	None
Abdominal pain	4 (26.67%)	1 (6.7%)
Flu-like symptoms	4 (26.67%)	1 (6.7%)
Cough	4 (26.7%)	None
Nausea	4 (26.7%)	None
Bilirubin increase	3 (20.0%)	1 (6.7%)
Mucositis	3 (20.0%)	None
Dysgeusia	3 (20.0%)	None
Hypothyroidism	3 (20.0%)	None
Upper respiratory infection	3 (20.0%)	None